

# Donor-acceptor copolymer based on dioctylporphyrin: Synthesis and application in organic field-effect transistors

Xiaochen Wang<sup>a</sup>, Yugeng Wen<sup>b</sup>, Hao Luo<sup>b</sup>, Gui Yu<sup>b,\*</sup>, Xiaoyu Li<sup>a,\*</sup>, Yunqi Liu<sup>b,\*</sup>, Haiqiao Wang<sup>a,\*</sup>

<sup>a</sup>State Key Laboratory of Organic–Inorganic Composites, College of Materials Science and Engineering, Beijing University of Chemical Technology, Beijing 100029, China

<sup>b</sup>Beijing National Laboratory for Molecular Sciences, Institute of Chemistry, Chinese Academy of Sciences, Beijing 100190, China

## ARTICLE INFO

### Article history:

Received 16 December 2011

Received in revised form

28 February 2012

Accepted 7 March 2012

Available online 13 March 2012

### Keywords:

Porphyrin

Donor-acceptor copolymer

Organic field-effect transistors

## ABSTRACT

A novel alternating D–A copolymer, **PPor–BT**, with dioctylporphyrin (**Por**) as a donor unit and 5,6-bis(octyloxy)benzo-2,1,3-thiadiazole (**BT**) as an acceptor unit, was designed and synthesized by Pd-catalyzed Sonogashira-coupling reaction. The copolymer showed good solubility and film-forming ability. **PPor–BT** exhibited a broad absorption band from 350 to 950 nm with two peaks centered at 456 and 818 nm corresponding to the Soret band and Q-bands absorption of porphyrin segments, respectively. The employment of electron deficient **BT** unit to construct donor-acceptor structure observably broadened the absorption spectrum and enhanced the Q-band absorption of the porphyrin-based polymer. The HOMO and LUMO energy levels of the polymer are  $-5.06$  eV and  $-3.63$  eV, respectively. The solution-processed organic field-effect transistors (OFETs) were fabricated with bottom gate/top-contact geometry. The mobility of **PPor–BT** based OFETs reached  $4.3 \times 10^{-5} \text{ cm}^2 \text{ V}^{-1} \text{ s}^{-1}$  with an on/off current ratio of  $10^4$ . This mobility is among the highest values for porphyrin-based polymers.

© 2012 Elsevier Ltd. All rights reserved.

## 1. Introduction

Porphyrin derivatives have been intensively studied over the past century because of their unique nature. The porphyrin is a heterocyclic macrocycle derived from four pyrroline subunits interconnected via their  $\alpha$ -carbon atoms via methine bridges [1]. The macrocycle is a highly-conjugated system with deep color. The name porphyrin comes from a Greek word for purple. In recent years, porphyrin molecules and relative polymers have attracted tremendous interest due to their potential applications in optoelectronic devices, such as organic light emitting diodes [2–9], organic field-effect transistors (OFETs) [10–14], and organic solar cells [14–20].

The performances of organic semiconductors rely on the inherent structural uniqueness, such as planarity, conjugation, and their packing and intermolecular interactions. In this regard, porphyrins would be one of the best candidates for organic transistors because of their multiple inter- and/or intramolecular interactions, such as  $\pi$ – $\pi$  stacking, electrostatic interactions, as well as metal–ligand coordination, in different derivatives [21]. OFET devices based on small porphyrin molecules exhibit carrier

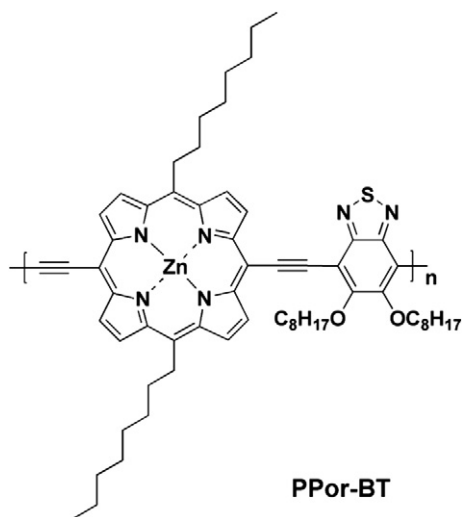
mobilities up to  $0.32 \text{ cm}^2 \text{ V}^{-1} \text{ s}^{-1}$  [11]. However, there have been only a few reports about porphyrin-containing polymers used in OFETs as active layers [10,14]. Performances of porphyrin-based polymer transistors are quite poor. For example, porphyrin–diacetylene polymer transistors only showed mobilities of  $10^{-7} \text{ cm}^2 \text{ V}^{-1} \text{ s}^{-1}$  at room temperature [10].

Recently, considerable attention has been focused on donor-acceptor (D–A) conjugated copolymers, where electron-rich and electron deficient units are polymerized in an alternating fashion along the polymer backbone, because their electronic and optoelectronic properties could be efficiently tuned by intramolecular charge transfer (ICT) [22–31]. The hybridization of the highest occupied molecular orbital (HOMO) on the donor moiety and the lowest unoccupied molecular orbital (LUMO) on the acceptor moiety provides a method to tune the electronic and optoelectronic properties for various needs. High carrier mobilities were obtained from the D–A copolymer systems through the manipulation of intramolecular charge transfer, morphology, or gate dielectric surface modification [27–29]. Among those well investigated acceptors, 2,1,3-benzothiadiazole (**BT**) unit has previously been proven to enhance  $\pi$ -stacking morphologies, leading to high charge carrier mobility [32].

Here we designed and synthesized a novel alternating D–A copolymer, **PPor–BT**, with 5,15-dioctylporphyrin (**Por**) as donor unit, and 5,6-bis(octyloxy)benzo-2,1,3-thiadiazole (**BT**) as acceptor unit. The structure of **PPor–BT** is shown in Scheme 1. In this

\* Corresponding authors. Tel.: +86 010 64419631.

E-mail addresses: yug@iccas.ac.cn (G. Yu), lixy@mail.buct.edu.cn (X. Li), liuyq@iccas.ac.cn (Y. Liu), wanghaiqiao@mail.buct.edu.cn (H. Wang).



Scheme 1. Molecular structure of PPor-BT.

contribution, the 5,15-dioctylporphyrin unit was used to enhance both the coplanarity of the molecular backbone and the  $\pi$ - $\pi$  stacking in the solid state of the copolymer, while the electron deficient BT unit was employed to construct donor-acceptor structure, which would facilitate high-performance OFETs [27–29]. In addition, the well-defined alternating D–A structure of polymer combined with the linear alkyl side chains is expected to optimize the molecular packing in the solid state. OFETs based on the polymer were fabricated and characterized. The highest hole mobility of PPor-BT reached  $4.3 \times 10^{-5} \text{ cm}^2 \text{ V}^{-1} \text{ s}^{-1}$  with an ON/OFF current ratio of  $10^4$ .

## 2. Experimental section

### 2.1. Measurements and characterization

The molecular weight of the polymer was measured by gel permeation chromatography (GPC) method. The GPC measurements were performed on Waters 515-2410 with polystyrenes as reference standard and tetrahydrofuran (THF) as an eluent. All new compounds were characterized by nuclear magnetic resonance spectra (NMRs) and/or Mass spectra (MS). The NMRs were recorded on a Bruker AV 600 spectrometer in  $\text{CDCl}_3$  or THF at room temperature. Chemical shifts of  $^1\text{H}$  NMR were reported in ppm. Splitting patterns were designated as s (singlet), d (doublet), t (triplet), m (multiplet), and br (broaden). Mass spectra were measured on a GCT-MS micromass (U.K.) spectrometer using the electron impact (EI) mode or on a Bruker Daltonics BIFLEX III MALDI-TOF Analyzer using MALDI mode. Elemental analyses were performed on a Flash EA 1112 analyzer. UV-Vis absorption spectra were recorded on a Shimadzu spectrometer model UV-3150. Absorption spectrum measurement of the polymer solution was carried out in THF (analytical reagent) at 25 °C. Absorption spectrum measurement of the polymer film was carried out on the quartz plates with the polymer film spin-coated from the polymer solution in THF (analytical reagent) at 25 °C. The electrochemical cyclic voltammetry was conducted on a Zahner IM6e electrochemical workstation with a Pt plate, Pt wire, and  $\text{Ag}/\text{Ag}^+$  electrode as the working electrode, counter electrode, and reference electrode, respectively, in a 0.1 mol/L tetrabutylammonium hexafluorophosphate ( $\text{Bu}_4\text{NPF}_6$ ) acetonitrile solution. Polymer thin films were formed by drop-casting polymer solutions in THF (analytical reagent) on the working electrode and were then dried in air. X-Ray

diffraction (XRD) measurements of thin films were performed in reflection mode at 40 kV and 200 mA with Cu-K $\alpha$  radiation using a 2 kW Rigaku X-ray diffractometer. Atomic force microscopy (AFM) images of the thin films were obtained on a Nanoscope IIIa AFM (Digital Instruments) operating in tapping mode.

### 2.2. Fabrication of field-effect transistor

OFETs were fabricated on highly doped silicon substrates with thermally grown 300-nm-thick silicon oxide ( $\text{SiO}_2$ ) insulating layer, where the substrate served as a common gate electrode. Prior to polymer semiconductor deposition, the substrates were treated with the silylating agent octyltrichlorosilane (OTS). Thin semiconductor films were then deposited by spin-coating the polymer solutions in chlorobenzene:THF (1:1) on the substrates. The film thickness was measured by an XP-2 surface profilometer (Ambios Technology). The samples were then dried and annealed at 140 °C under nitrogen. Source-drain gold electrodes were deposited on the polymer layer by vacuum evaporation under  $7 \times 10^{-4}$  Pa to form top-contact geometry. The electrical characterization of the transistor devices was performed using a Keithley 4200 semiconductor parameter analyzer.

## 3. Synthesis of the monomers

### 3.1. Dipyrromethane (2)

Formaldehyde gas (generated by cracking paraformaldehyde (35 g, 1.16 mol) at 160 °C) passed into an oxygen-free solution of TFA (13.68 g, 0.12 mol) in pyrrole (2 L, 30 mol) under a slow flow of nitrogen. After all the paraformaldehyde had been transferred, the reaction mixture was stirred at room temperature for another 30 min. The resulting yellow solution was washed with 10% NaOH solution before distilled to remove excess pyrrole. Then the crude product was purified by column chromatography (petroleum ether: EtOAc:  $\text{Et}_3\text{N}$  100: 10: 1) to afford the product as a white crystal (71 g, 42%).  $^1\text{H}$  NMR (600 MHz,  $\text{CDCl}_3$ ):  $\delta$  7.90 (br, 2H), 6.69 (s, 2H), 6.17 (d, 2H), 6.06 (s, 2H), 4.00 (s, 2H). ESI-MS:  $m/z = 147.1$  ( $\text{M}^+ + 1$ ).

### 3.2. 5,15-Dioctylporphyrin (3)

A solution of 1-decyne (0.684 g, 4.8 mmol) and dipyrromethane (0.702 g, 4.8 mmol) in  $\text{CH}_2\text{Cl}_2$  (1 L) was purged with nitrogen for 30 min, and then trifluoroacetic acid (TFA) (0.3 g, 2.6 mmol) was added. The mixture was stirred for 3 h at room temperature, and then DDQ (1.84 g, 8 mmol) was added. After the mixture was stirred at room temperature for an additional 30 min, the reaction was quenched by adding triethylamine (2 mL). The solvent was removed, and the residue was purified by column chromatography on silica gel using dichloromethane/petroleum ether as the eluent. Recrystallization from dichloromethane/ethanol gave a purple solid (0.40 g, 31%).  $^1\text{H}$  NMR (600 MHz,  $\text{CDCl}_3$ ):  $\delta$  10.17 (s, 2H), 9.58 (d, 4H), 9.41 (d, 4H), 5.01 (t, 4H), 2.55 (m, 4H), 1.81 (m, 4H), 1.55 (m, 4H), 1.37 (m, 4H), 1.30 (m, 8H), 0.88 (t, 6H),  $-2.92$  (br, 2H). MALDI-TOF:  $m/z = 535.5$  ( $\text{M}^+$ ).

### 3.3. 5,15-Dibromo-10,20-dioctylporphyrin (4)

Porphyrin 3 (2.86 g, 4.4 mmol) was dissolved in 300 mL chloroform (40 mL), and then NBS (1.60 g, 9 mmol) was added.

After stirring for 3 h, the reaction was quenched by addition of acetone (10 mL). The solvents were removed, and the residue was washed with ethanol three times and then recrystallized from dichloromethane/ethanol to afford a purple solid (3.13 g, 88%).  $^1\text{H}$  NMR (600 MHz,  $\text{CDCl}_3$ ):  $\delta$  9.80 (d, 4H), 9.49 (d, 4H), 4.94 (t, 4H), 2.51

(m, 4H), 1.79 (m, 4H), 1.52 (m, 4H), 1.31 (m, 12H), 0.88 (m, 6H), –2.87 (s, 2 H). MALDI-TOF:  $m/z = 693.4$  ( $M^+$ ).

### 3.4. 5,15-Dibromo-10,20-dioctylporphyrin zinc (5)

To a solution of compound **4** (0.81 g, 1 mmol) in dichloromethane (500 mL) was added a solution of  $Zn(OAc)_2 \cdot H_2O$  (1.1 g, 5 mmol) in methanol (30 mL). The reaction mixture was stirred at room temperature over night. Evaporation of the solvent and washing three times with ethanol afforded a purple solid without further purification.

### 3.5. 5,15-Bis(trimethylsilylethynyl)-10,20-dioctylporphyrin zinc (6)

Compound **5** (0.87 g, 1 mmol) was dissolved in THF (100 mL) and triethylamine (50 mL) was added. The mixture was purged with nitrogen for 10 min. Then  $Pd(PPh_3)_2Cl_2$  (35 mg, 0.05 mmol), CuI (10 mg, 0.05 mmol), and trimethylsilylacetylene (0.4 g, 5 mmol) were added. Then the mixture was purged with nitrogen for another 15 min. After stirring at room temperature for 3 days under nitrogen, the solvent was removed under reduced pressure. The residue was purified by column chromatography (silica gel,  $CH_2Cl_2$ /petroleum ether) to afford a purple solid (0.624 g, 79%).  $^1H$  NMR (600 MHz,  $CDCl_3$ ):  $\delta$  9.49 (s, 4H), 9.22 (s, 4H), 4.69 (s, 4H), 2.35 (t, 4H), 1.76 (m, 4H), 1.51 (m, 4H), 1.42 (m, 8H), 1.11 (m, 4H), 0.90 (m, 6H), 0.61 (s, 18H).

### 3.6. 5,15-Diethynyl-10,20-dioctylporphyrin zinc (Por)

Tetrabutylammonium fluoride (0.88 g, 75% in water) was added to a stirred solution of porphyrin **6** (1.00 g, 1.26 mmol) in THF (100 mL). After stirring for 30 min, water was added to quench the reaction. The solution was extracted with chloroform, washed with water and dried over anhydrous  $MgSO_4$ . After evaporation of the solvent, the residue was recrystallized from dichloromethane/ethanol to afford a purple solid (0.55 g, 67%).  $^1H$  NMR (600 MHz,

THF- $d_6$ ):  $\delta$  10.83 (s, 2H), 9.68 (d, 4H), 9.55 (s, 4H), 5.01 (t, 4H), 2.52 (m, 4H), 1.81 (m, 4H), 1.53 (m, 4H), 1.38 (m, 4H), 1.36 (m, 8H), 0.89 (m, 6H). MALDI-TOF:  $m/z = 645.1$  ( $M^+$ ).

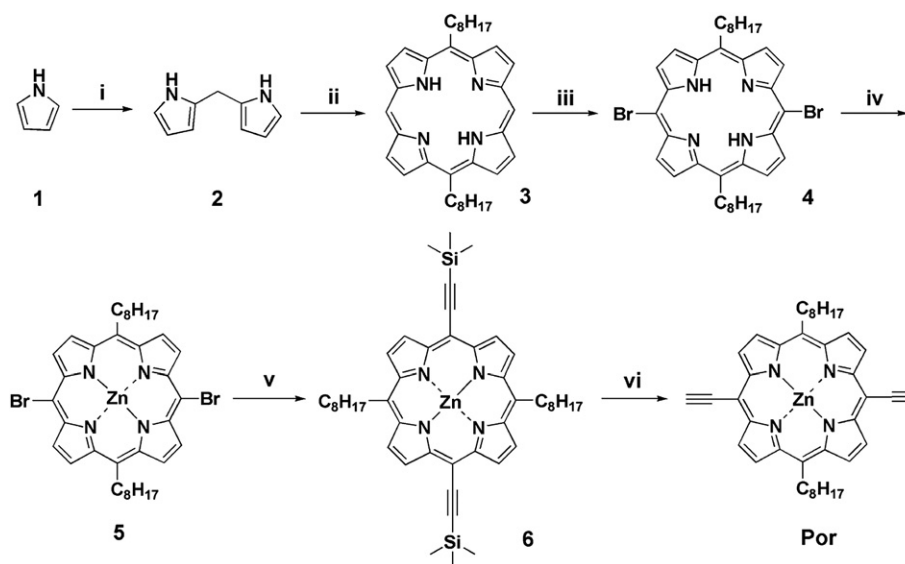
### 3.7. Synthesis of the polymer

**Por** monomer (324 mg, 0.5 mmol) and **BT** monomer (275 mg, 0.5 mmol) were put into a 100 mL two-neck flask, then 40 mL of toluene and 20 mL triethylamine were added. The mixture was stirred and purged with nitrogen for 10 min, and then  $Pd(PPh_3)_4$  (30 mg, 0.025 mmol), CuI (19 mg, 0.1 mmol) was added. After being purged for another 15 min, the mixture was heated at 60 °C for 48 h. The terminal bromobenzene and phenylacetylene were added as end cappers, with the phenylacetylene added first and the bromobenzene added 12 h later. After stirring for another 12 h, the reaction solution was cooled to room temperature. Then the reaction mixture was added dropwise to 400 mL methanol, then collected by filtration and washed with methanol. The black solid was filtered into a Soxhlet funnel and extracted by methanol, hexane, chloroform and THF successively. The polymer was recovered from THF fraction and dried under vacuum for 1 day to afford the target polymer **PPor–BT** as a black solid. (yield 41%,  $M_n = 7.5$  kDa,  $M_w = 16.7$  kDa, PDI = 2.2).  $^1H$  NMR ( $CDCl_3$ , 600 MHz):  $\delta$  10.00 (br, 4H), 9.71 (br, 4H), 5.11 (br, 4H), 4.27 (br, 4H), 2.49 (br, 4H), 2.00–0.91 (br, 56H). Anal. Calcd for  $(C_{62}H_{76}N_6O_2SZn)_n$ : C, 71.90; H, 7.34; N, 8.12. Found: C, 71.42; H, 7.48; N, 8.09.

## 4. Results and discussion

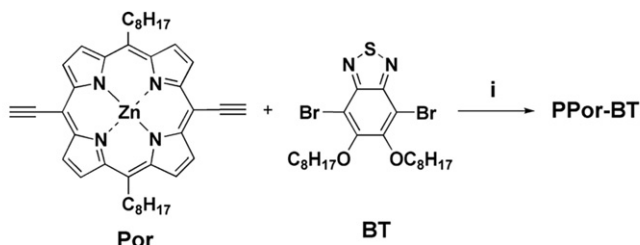
### 4.1. Syntheses of monomers and polymer

The synthetic routes of monomers and corresponding polymer are outlined in Schemes 2 and 3, respectively. Monomer BT was synthesized according to our previously proposed procedure [33]. Dipyrromethane **2** was synthesized by condensation of pyrrole with formaldehyde, which was generated by cracking



<sup>a</sup>Reagents, conditions and yields: (i)  $CH_2O$ , TFA, 42%; (ii) 1-Decyne, TFA, then DDQ, 31%; (iii) NBS,  $CHCl_3$ , 88%; (iv) zinc acetate,  $CH_2Cl_2$ ,  $CH_3OH$ ; (v) TMSA,  $Pd(PPh_3)_2Cl_2$ , CuI, THF,  $Et_3N$ , 79%; (vi) TBAF, THF, 67%.

Scheme 2. Synthetic routes of the monomers.<sup>a</sup>



<sup>a</sup>Reagents, conditions and yields:(i) Pd(PPh<sub>3</sub>)<sub>4</sub>, THF, Et<sub>3</sub>N, 60°C, 48h, 41%.

Scheme 3. Synthetic route of the polymer<sup>a</sup>.

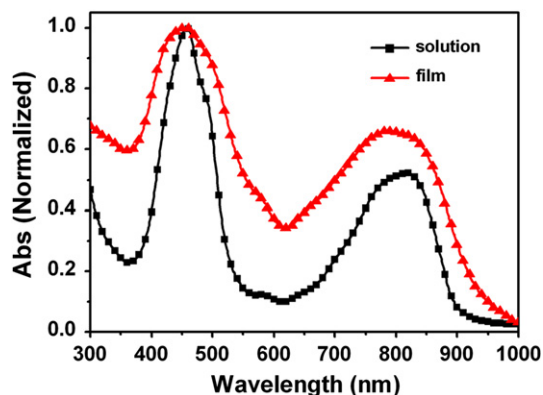


Fig. 1. Normalized absorption spectra of the **PPor-BT** in THF solution and film on a quartz plate.

paraformaldehyde at 160 °C, in the presence of TFA. New intermediate *trans*-substituted porphyrin **3** was synthesized in 31% yield by acid-catalyzed condensation of dipyrromethane with 1-decyne, followed by oxidation with 2, 3-dichloro-5,6-dicyano-1,4-benzoquinone (DDQ) at room temperature, similar to Lindsey's method [34]. Coordination reaction with zinc acetate after bromination of **3** with NBS was taken to obtain zinc dibromoporphyrin **5** in high yield. Monomer diethynylporphyrin **6** was synthesized by Sonogashira-coupling reaction between zinc dibromoporphyrin **5** and trimethylsilylacetylene (TMSA) in high yield. Finally, the protecting trimethylsilyl groups were removed with tetrabutylammonium fluoride (TBAF) in room temperature to afford **Por**. All new compounds have been characterized by NMR and/or MS. The data are consistent with the proposed structures. The synthesis of the polymer was carried out using palladium-catalyzed Sonogashira-coupling between monomer **Por** and **BT**. All starting materials, reagents, and solvents were carefully purified, and all procedures were performed under an air-free environment. The structure of the polymer was confirmed by <sup>1</sup>H NMR spectroscopy and elemental analysis. **PPor-BT** has reasonable solubility in common organic solvents such as THF, chlorobenzene and *o*-dichlorobenzene. It can be readily processed to form smooth and pinhole-free films upon spin-coating.

Table 1  
Optical properties of **PPor-BT**.

<b>PPor-BT</b>	$\lambda_{\text{abs}}$ (nm)	$\lambda_{\text{onset}}$ (nm)	$E_g^{\text{opt}}$ (eV) <sup>a</sup>
In THF	457, 818	899	—
In films	454, 790	925	1.34

<sup>a</sup> Band gap estimated from the onset wavelength ( $\lambda_{\text{onset}}$ ) of the optical absorption:  $E_g^{\text{opt}} = 1240/\lambda_{\text{onset}}$ .

## 4.2. Optical properties

Fig. 1 shows the absorption spectra of the polymer in THF solution and solid thin film on a quartz plate. Table 1 summarizes the optical data, including the absorption peak wavelengths ( $\lambda_{\text{abs}}$ ), absorption edge wavelengths ( $\lambda_{\text{onset}}$ ), and the optical band gap ( $E_g^{\text{opt}}$ ). In THF solution, the polymer exhibited two peaks centered at 456 and 818 nm, which is a typical absorption profile of Soret band and Q-bands for porphyrin compounds. In solid film, the absorption spectrum was expanded to 950 nm with an enhanced Q-band due to the aggregation of the porphyrin rings. The optical band gap determined from onset of the absorption of **PPor-BT** film was 1.34 eV. Compared with other porphyrin derivatives based polymers, **PPor-BT** exhibited very broad absorption spectrum and extremely

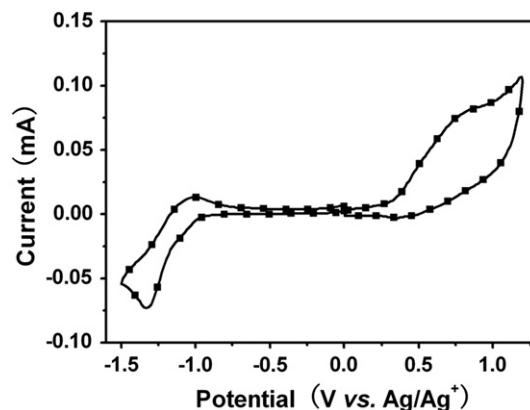


Fig. 2. Cyclic voltammogram of the polymer film on Pt electrode in 0.1 mol/L Bu<sub>4</sub>NPF<sub>6</sub>, CH<sub>3</sub>CN solution with a scan rate of 100 mV/s.

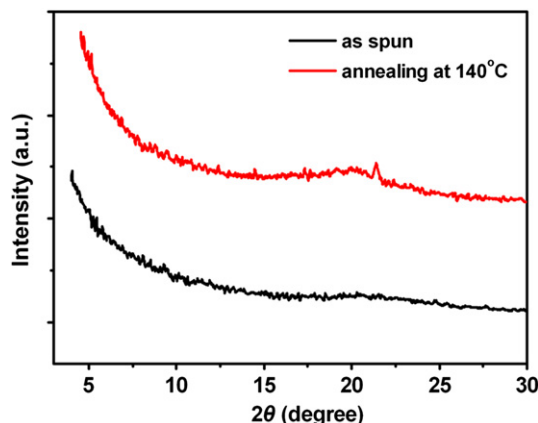


Fig. 3. XRD images of spin-coated films.

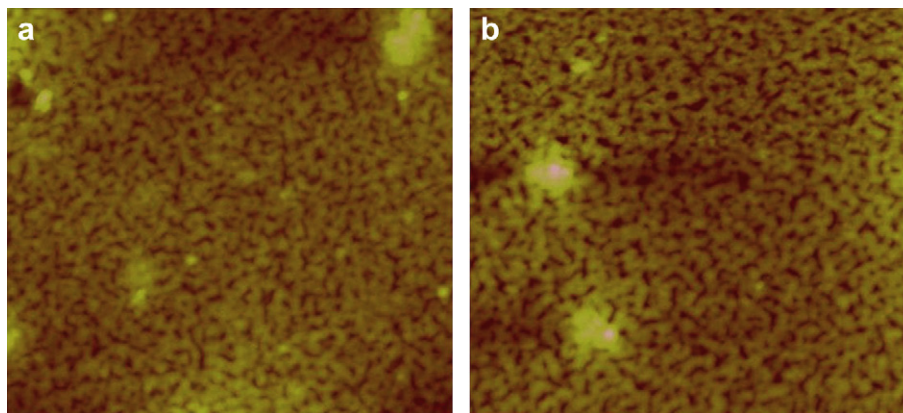


Fig. 4. AFM images ( $2 \times 2 \mu\text{m}^2$ ) of spin-coated films: (a) before and (b) after annealing at  $140^\circ\text{C}$ .

strong Q-band absorption. This is benefit from intramolecular charge transfer between the **Por** and **BT** moieties. These results demonstrate that the employment of electron deficient **BT** unit to construct donor-acceptor structure can observably broaden the absorption spectrum and enhance the Q-band absorption of porphyrin-based polymers.

#### 4.3. Electrochemical properties

Cyclic voltammetry has been employed and considered as an effective tool in investigating electrochemical properties of conjugated oligomers and polymers [35]. From the onset oxidation and reduction potentials in the cyclic voltammogram, energy levels of HOMO and the lowest unoccupied molecular orbital (LUMO) can be readily estimated, which correspond to ionization potential (IP) and electron affinity (EA), respectively [9].

Cyclic voltammogram of the polymer film is shown in Fig. 2. The onset oxidation potential ( $E_{\text{ox}}$ ) and onset reduction potential ( $E_{\text{red}}$ ) of **PPor–BT** are  $0.35 \text{ V vs. Ag/Ag}^+$  and  $-1.08 \text{ V vs. Ag/Ag}^+$  respectively. The HOMO and LUMO energy levels of the polymer are calculated from the onset oxidation potential and the onset reduction potential according to the equations [36]:

$$\text{HOMO} = -e(E_{\text{ox}} + 4.71)(\text{eV})$$

$$\text{LUMO} = -e(E_{\text{red}} + 4.71)(\text{eV})$$

The calculated HOMO and LUMO energy levels of the polymer are  $-5.06 \text{ eV}$  and  $-3.63 \text{ eV}$ , respectively. The electrochemical band gap of the polymer ( $E_{\text{g}}^{\text{opt}} = 1.43 \text{ eV}$ ) is well matched with its optical band gap within the experimental error.

#### 4.4. Film morphology and characteristics

The morphology and crystalline characteristics of the spin-coated films of the polymer with or without annealing were investigated by X-ray diffraction (XRD) and atomic force microscopy (AFM), respectively. Fig. 3 shows the XRD patterns of spin-coated thin films of **PPor–BT**. It can be observed that the as-spun film is amorphous, and the annealed film shows clear peaks, which is indicative of improved molecular ordering. As shown in the AFM images (Fig. 4), the morphology of the thin films undergoes obvious changes with annealing. When annealed at  $140^\circ\text{C}$  for 2 h, the grain size increased and thus the mobility improved.

#### 4.5. Field-effect transistor properties of the polymer

Fig. 5 shows the typical output and transfer curves of OFET device with **PPor–BT** as the active layer. The performances of the polymer based devices are summarized in Table 2. The output behavior closely followed the metal-oxide semiconductor FET gradual-channel model with very good saturation (Fig. 5a). The transfer characteristics of **PPor–BT** based devices showed a low drain current at zero gate voltage (Fig. 5b), which shows its high air stability due to the low HOMO ( $-5.06 \text{ eV}$ ) energy level. Without

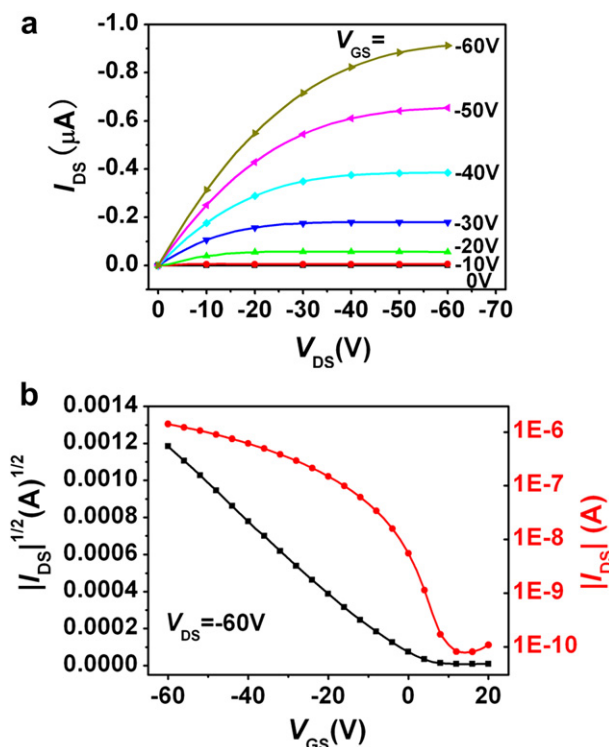


Fig. 5. (a) Output and (b) transfer characteristics of top-contact OFET using **PPor–BT** as the active layer (annealed at  $140^\circ\text{C}$ ).

Table 2

FET properties of devices with the polymer films spin-coated on OTS-Modified  $\text{SiO}_2/\text{Si}$  substrates.

<b>PPor–BT</b>	$\mu$ ( $\text{cm}^2/\text{V}\cdot\text{s}$ )	$I_{\text{on}}/I_{\text{off}}$	$V_{\text{Th}}(\text{V})$
Without annealing	$1.3 \times 10^{-6}$	140	0
Annealed at $140^\circ\text{C}$	$4.3 \times 10^{-5}$	$10^4$	2

annealing, the OFET with **PPor–BT** as the active layer showed a mobility of  $1.3 \times 10^{-6} \text{ cm}^2/\text{V}\cdot\text{s}$  in the saturation regime, together with an on/off ratio of 140 when measured under ambient conditions. Annealing the devices at 140 °C for 30 min led to improved charge carrier mobility of up to  $4.3 \times 10^{-5} \text{ cm}^2 \text{ V}^{-1} \text{ s}^{-1}$  with an on/off current ratio of  $10^4$  and a threshold voltage ( $V_{\text{TH}}$ ) of 2 V. The charge carrier mobility is two orders of magnitude higher than that of non-D–A porphyrin–diacetylene copolymer [10]. These results demonstrate that carrier mobility of porphyrin-based conjugated polymers could be efficiently increased by intramolecular charge transfer. High carrier mobilities could be obtained from porphyrin-based D–A copolymer systems through the manipulation of intramolecular charge transfer.

## 5. Conclusion

We designed and synthesized a novel porphyrin-based polymer-DPP (**PPor–BT**). The polymer demonstrated good solubility in common organic solvents and broad absorption spectrum with extremely enhanced Q-band absorption. The HOMO and LUMO energy levels of the polymer are  $-5.06 \text{ eV}$  and  $-3.63 \text{ eV}$ , respectively. The solution-processed organic field-effect transistors were fabricated with bottom gate/top-contact geometry. The hole mobility of **PPor–BT** reached  $4.3 \times 10^{-5} \text{ cm}^2 \text{ V}^{-1} \text{ s}^{-1}$  with an on/off current ratio of  $10^4$ . This mobility is one of the highest values for porphyrin-based polymers. These results demonstrate that electronic and optoelectronic properties of porphyrin-based conjugated copolymers could be efficiently tuned by intramolecular charge transfer. High FET carrier mobilities could be obtained from porphyrin-based D–A copolymer systems through the manipulation of intramolecular charge transfer. Most importantly, this work opens up a new path to design high-performance porphyrin-based materials.

## Acknowledgments

This work was supported by Beijing Natural Science Foundation (No. 2122047). We thank Professor Yongfang Li for his help with the CV measurements.

## References

- [1] Nardi M, Verucchi R, Corradi C, Pola M, Casarin M, Vittadini A, et al. *Phys Chem Chem Phys* 2010;12:871–80.
- [2] Burrows PE, Forrest SR, Sibley SP, Thompson ME. *Appl Phys Lett* 1996;69:2959–61.
- [3] Baldo MA, O'Brien DF, You Y, Shoustikov A, Sibley S, Thompson ME, et al. *Nature* 1998;395:151–4.
- [4] Iqbal R, Yahioğlu G, Milgrom L, Moratti SC, Holmes AB, Cacialli F, et al. *Synthetic Met* 1999;102:1024–5.
- [5] Morgado J, Cacialli F, Iqbal R, Moratti SC, Holmes AB, Yahioğlu G, et al. *J Mater Chem* 2001;11:278–83.
- [6] Morgado J, Cacialli F, Friend RH, Iqbal R, Yahioğlu G, Milgrom LR, et al. *Chem Phys Lett* 2000;325:552–8.
- [7] Virgili T, Lidzey DG, Bradley DDC. *Adv Mater* 2000;12:58–62.
- [8] (a) Li BS, Li J, Fu YQ, Bo ZS. *J Am Chem Soc* 2004;126:3430–1; (b) Li CH, Bo ZS. *Polymer* 2010;51:4273–94.
- [9] Wang XC, Wang HQ, Yang Y, He YJ, Zhang L, Li YF, et al. *Macromolecules* 2010;43:709–15.
- [10] Pichler K, Anderson HL, Bradley DDC, Friend RH, Hamer PJ, Harrison MG, et al. *Mol Cryst Liq Cryst* 1994;256:415–22.
- [11] Hoang MH, Kim Y, Kim SJ, Choi DH, Lee SJ. *Chem Eur J* 2011;17:7772–6.
- [12] Noh YY, Kim JJ, Yoshida Y, Yase K. *Adv Mater* 2003;15:699–702.
- [13] Shea PB, Kanicki J, Pattison LR, Petroff P, Kawano M, Yamada H, et al. *J Appl Phys* 2006;100:034502–8.
- [14] Huang XB, Zhu CL, Zhang SN, Li WW, Guo YL, Zhan XW, et al. *Macromolecules* 2008;41:6895–902.
- [15] Wang CL, Zhang WB, Van Horn RM, Tu YF, Gong X, Cheng SZD, et al. *Adv Mater* 2011;23:2951–6.
- [16] Zhan HM, Lamare S, Ng A, Kenny T, Guernon H, Chan WK, et al. *Macromolecules* 2011;44:5155–67.
- [17] Bessho T, Zakeeruddin SM, Yeh CY, Diau EWG, Gratzel M. *Angew Chem Int Ed* 2010;49:6646–9.
- [18] Fukuzumi S, Kojima T. *J Mater Chem* 2008;18:1427–39.
- [19] Perez MD, Borek C, Djurovich PI, Mayo EI, Lunt RR, Forrest SR, et al. *Adv Mater* 2009;21:1517–20.
- [20] Liu YJ, Guo X, Xiang N, Zhao B, Huang H, Li H, et al. *J Mater Chem* 2010;20:1140–6.
- [21] (a) Zang L, Che Y, Moore JS. *Acc Chem Res* 2008;41:1596–608; (b) Laschat S, Baro A, Steinke N, Giesselmann F, Hgele C, Scalia G, et al. *Angew Chem Int Ed* 2007;46:4832–87.
- [22] (a) Li G, Shrotriya V, Huang J, Yao Y, Moriarty T, Emery K, et al. *Nat Mater* 2005;4:864–8; (b) Kim Y, Cook S, Tuladhar SM, Choulis SA, Nelson J, Durrant JR, et al. *Nat Mater* 2006;5:197–203; (c) Peet J, Kim JY, Coates NE, Ma WL, Moses D, Heeger AJ, et al. *Nat Mater* 2007;6:497–500.
- [23] Sivula K, Ball ZT, Watanabe N, Frechet JMJ. *Adv Mater* 2006;18:206–10.
- [24] (a) Ego C, Marsitzky D, Becker S, Zhang J, Grimsdale AC, Mullen K, et al. *J Am Chem Soc* 2003;125:437–43; (b) Liu J, Guo X, Bu LJ, Xie ZY, Cheng YX, Geng YH, et al. *Adv Funct Mater* 2007;17:1917–25.
- [25] Scharber MC, Muhlbacher D, Koppe M, Denk P, Waltauf C, Heeger AJ, et al. *Adv Mater* 2006;18:789–94.
- [26] Peng Q, Peng JB, Kang ET, Neoh KG, Cao Y. *Macromolecules* 2005;38:7292–8.
- [27] Chua LL, Zaumseil J, Chang JF, Ou ECW, Ho PKH, Sirringhaus H, et al. *Nature (London)* 2005;434:194–9.
- [28] (a) Babel A, Jenekhe SA. *J Am Chem Soc* 2003;125:13656–7; (b) Babel A, Zhu Y, Cheng KF, Chen WC, Jenekhe SA. *Adv Funct Mater* 2007;17:2542–9.
- [29] Zhu Y, Champion RD, Jenekhe SA. *Macromolecules* 2006;39:8712–9.
- [30] Thompson BC, Kim YG, McCarley TD, Reynolds JR. *J Am Chem Soc* 2006;128:12714–25.
- [31] Sonmez G, Shen CKF, Rubin Y, Wudl F. *Angew Chem Int Ed* 2004;43:1498–502.
- [32] (a) Tsao HN, Cho D, Andreasen JW, Rouhanipour A, Breiby DW, Pisula W, et al. *Adv Mater* 2009;21:209–12; (b) Zhang WM, Smith J, Watkins SE, Gysel R, McGehee M, Salleo A, et al. *J Am Chem Soc* 2010;132:11437–9.
- [33] (a) Wang XC, Sun YP, Chen S, Guo X, Zhang MJ, Li XY, et al. *Macromolecules* 2012;45:1208–16; (b) Wang XC, Chen S, Sun YP, Zhang MJ, Li YF, Li XY, et al. *Polym Chem* 2011;2:2872–7.
- [34] Lindsey JS, Prathapan S, Johnson TE, Wagner RW. *Tetrahedron* 1994;50:8941–68.
- [35] Li YF, Cao Y, Gao J, Wang DL, Yu G, Heeger AJ. *Synthetic Met* 1999;99:243–8.
- [36] (a) Sun QJ, Wang HQ, Yang CH, Li YF. *J Mater Chem* 2003;13:800–6; (b) Wang XC, Luo H, Sun YP, Zhang MJ, Li XY, Yu G, et al. *J Polym Sci Part A: Polym Chem* 2012;50:371–7.